P-ISSN 2586-9000
E-ISSN 2586-9027
Homepage : https://tci-thaijo.org/index.php/SciTechAsia
Science & Technology Asia
Vol. 28 No.1 January - March 2023
Page: [33-47]
Original research article

Time-Dependent Magneto-Convective Thermal-Material Transfer by Micropolar Binary Mixture Fluid Passing a Vertical Surface

Mosharrof Hossain[1,2], Hasanuzzaman[2], M.M.T. Hossain[2], R. Nasrin[3,*]

[1]*Department of Mathematics, Govt. BM College, Barishal 8200, Bangladesh*
[2]*Department of Mathematics, Khulna University of Engineering and Technology, Khulna 9203, Bangladesh*
[3]*Department of Mathematics, Bangladesh University of Engineering and Technology, Dhaka 1000, Bangladesh*

Received 28 June 2021; Received in revised form 28 October 2022
Accepted 7 November 2022; Available online 20 March 2023

ABSTRACT

Time-dependent magneto-convective thermal-material transport by micropolar binary mixture passing a vertical permeable surface with chemical reaction, radiative heat transfer and thermophoresis has been studied numerically. The findings of this study have significant industrial applications in the production of molten polymers, pulps, fossil fuels, and fluids containing certain additives, etc. Applying the similarity analysis together with Boussinesq estimate, the governing PDEs have been modified into ODEs. These equations have been solved by applying shooting technique with the help of "ODE45 MATLAB" software. The results of the numerical solutions of the problem involving velocity, temperature, concentration and micro-rotation are presented graphically for different dimensionless parameters and numbers, namely magnetic intensity, Damköhler number, thermophoresis, temperature dependent dynamic viscosity, thermal radiation, thermal Grashof number, solutal Grashof number, Prandtl number and Schmidt number. The magnetic intensity affects the velocity field only in the increase-decrease mode. An increase in Damköhler number and thermal radiation significantly enhances the velocity fields while interrupting the rate of heat transfer within the boundary layer. The temperature dependent dynamic viscosity greatly enhances the velocity of the fluid but reduces the micro-rotation of the particles very near to the wall. Also, the increase of Prandtl number lessens conduction of heat while increasing the micro-rotation of the particles noticeably very adjacent to the surface.

Keywords: Magneto-convection; Micropolar binary mixture fluid; Thermal-material transfer; Time-dependent; Vertical surface

***Corresponding author:** rehena@math.buet.ac.bd **doi:** 10.14456/scitechasia.2023.4

1. Introduction

In industries and engineering processes, many non-Newtonian fluids commonly flow along a vertical surface and are not possible to explain by a linear relationship between stress and rate of deformation. Molten polymers, fossils fuels, pulps, fluids and animal blood which contain assured preservatives, etc. are the examples of such fluids that sometimes are found in industrial production. The fluid dynamic researchers have given great attention to interpreting and explaining how these non-Newtonian fluids flow along vertical as well as horizontal stretching surfaces [1-3]. Furthermore, various inventive applications have been considered in areas of free convection. The adjacent fluids of a thermal resource region receive heat energy and become less dense which creates a tendency to rise for free convection. The cooler fluids in the surrounding region move forward to replace them [4]. These cooler fluids are further heated and this process continues to produce convection current. Through the whole process, heat energy is transferred from the hot portion of the fluid to the cool region [5]. The density difference due to the difference of temperature causes buoyancy which acts like a driving force in natural convection. Therefore, as the difference of temperature causes the differences in fluid density, acceleration force due to gravity is a very important component for the case of natural convection.

Using the flow model of a non-Newtonian power law fluid [6-7] studied the problems of free convection to investigate the characteristics of steady natural convection stream and thermal transport along a vertical surface (isothermal) using porous medium. Natural convective non-Newtonian flow passing an upright surface (corrugated) having consistent face temperature as well as uniform heat flux has been considered by among others [8, 9]. Degan et al. [10] conducted modified Darcy power-law model analytically in order to examine the transient natural convective non-Newtonian flow passing an upright surface using anisotropic permeable medium. Kumari and Jayanthi [11] and Rashad et al. [12] investigated mixed convective non-Newtonian flow along an upright surface filled with permeable medium.

Again, in several industries, it is observed that some binary mixtures of fluids may contain microstructure and the fluid having the property of skew-symmetric stress tensor is denoted as micropolar fluid. Bodily, rigid randomly oriented particles suspended in a viscous medium are found in micropolar fluids. Here the deformation of fluid particles is not considered. Bubbly liquids, ferrofluids, liquid crystals and blood flows, etc. are the physical examples of such micropolar fluids [13, 14]. Thermophoresis has received great interest due to its vast number of applications in the fields of deposition of radioactive particles, silicon thin films, particles impacting in gas turbines, nuclear reactors, and aerosol equipment. Thermophoresis or Thermo-migration is a phenomenon generally that refers to the phases of matter in gaseous mixtures, but most openly concerns aerosol mixtures. It is a system of migration of little particles in terms of falling the heat difference and an efficient technique for compilation of particles [15-16]. This phenomenon is observed in mixtures of colloidal particles where particle of dissimilar types exhibit different response by means of temperature gradient in macroscopic scale. In gas, if heat difference occurs, then little particles shift in the direction of lessening heat.

MHD of electrically conducting micropolar fluid is stumbled upon the sectors of geophysics, astrophysics, and in numerous manufacturing applications such as nuclear reactors, generators, geothermal energy extractions and plasma studies, etc. Unsteady MHD heat-mass transfer by micropolar mixture having heat radiation was investigated by Hayat and Qasim [17]. Hasanuzzaman et al. [18] explained the

effects of Dufour and thermal scattering on unstable free magnet-conductive heat-mass transport across infinitely vertical perforated sheets. Hasanuzzaman et al. [19] extended Hasanuzzaman et al. [18] by considering the additional term internal heat generation or absorption. They solved the ODEs by applying the shooting technique through the 'MATLAB ODE45' software. Animasaun [20] performed thermo-physical intensities on MHD non-Darcian Casson fluid flow through stretching upright surface having relocation of colloidal particles. More recently, applying modified Boussinesq approximation, Animasaun [21] further investigated the convective unsteady micropolar binary mixture passing an upright permeable surface. Under consideration of fixed vortex viscosity with thermophoresis, temperature dependent dynamic viscosity, chemical reaction and radiative thermal transport, numerical calculation has been carried out for velocity, temperature, concentration and micro-rotation profiles with the variations of some selected parameters, using fourth order R-K method together with shooting technique. Similar solutions of both steady and unsteady MHD boundary layer flow and heat transfer over a stretching surface and a moving wedge using the Buongiorno's nanofluid model were conducted by Ali et al. [22, 23].

In view of the above research works, the present study will carry out the numerical investigation of unsteady convective thermal and mass transport passing a vertical porous plate with thermophoresis, chemical reaction and radiative thermal transfer with uniform magnetic field by a micropolar fluid with binary mixture. Computations have been performed for a wide range of the non-dimensional parameters such as magnetic field, Prandtl number, modified solutal and thermal Grashof numbers, Schmidt number, Damköhler number, radiation, thermophoresis and variable viscosity and are discussed graphically.

2. Mathematical Analysis

An incompressible, unsteady, convective, tacky, optically thin (absorption coefficient $\alpha \ll 1$) and micropolar binary mixture flow past an upright permeable exterior has been conducted numerically in this research. Fig. 1 displays the flow of the binary mixture alongside the semi-infinite surface (x-axis) and perpendicular to this is denoted as y-axis. It is assumed that $\frac{\partial T}{\partial y} \gg \frac{\partial T}{\partial x}$. Using Boussinesq's approximation the boundary governing the flow, heat and mass transfer have been written in the following form according to Hossain et al. [24]:

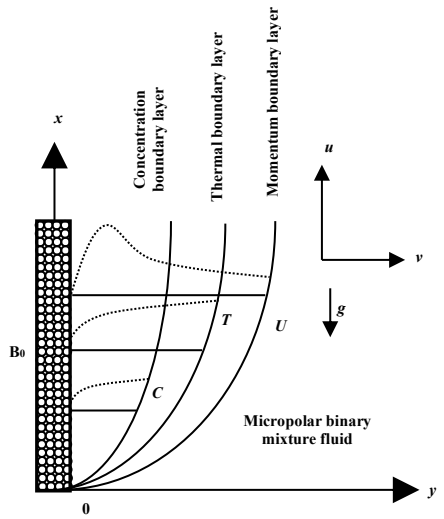

Fig. 1. Physical configuration and coordinate system of the problem.

The Continuity Equation

$$\frac{\partial v}{\partial y} = 0. \tag{2.1}$$

The Momentum Equation

$$\frac{\partial u}{\partial t} + v\frac{\partial u}{\partial y} = \left(\frac{\mu+\tau}{\rho}\right)\frac{\partial^2 u}{\partial y^2} + \frac{\tau}{\rho}\frac{\partial N}{\partial y} + g\beta\left(T - T_\infty\right) + g\beta^*\left(C - C_\infty\right) - \frac{\sigma B_0^2}{\rho}u. \tag{2.2}$$

Here a uniform transversed magnetic field B_0 is imposed along *y*-axis and there is no electric field. Thus, the Hall effect of MHDs is kept as disregarded.

The Energy Equation

$$\rho C_p\left(\frac{\partial T}{\partial t}+v\frac{\partial T}{\partial y}\right)=\kappa\frac{\partial^2 T}{\partial y^2}+Q-4\sigma\alpha^2T^4. \tag{2.3}$$

The Concentration Equation

$$\frac{\partial C}{\partial t}+v\frac{\partial C}{\partial y}+\frac{\partial}{\partial y}\left[V_T\left(C-C_\infty\right)\right]=D_m\frac{\partial^2 C}{\partial y^2}-R_A. \tag{2.4}$$

The Angular Momentum Equation

$$\frac{\partial N}{\partial t}+v\frac{\partial N}{\partial y}=\frac{\gamma^*}{\rho j}\frac{\partial^2 N}{\partial y^2}-\frac{\tau}{\rho j}\left(2N+\frac{\partial u}{\partial y}\right). \tag{2.5}$$

According to Cheng [25], the heat flux $\frac{\partial q_r}{\partial y}$ due to radiation is chosen as the fourth power of temperature in the Eq. (2.3); *v* is surely a time dependent function or constant in the continuity Eq. (2.1). According to Makinde [26], v can be written as

$$v=-c\left(\frac{v}{t}\right)^{\frac{1}{2}}. \tag{2.6}$$

Here the injection and suction are represented by $c < 0$ and > 0, respectively. According to [27, 28] the viscosity (spin gradient) and micro-inertia (per unit mass) may be assumed as follows:

$$j=\frac{\mu}{\rho U_0}\quad\text{and}\quad\gamma^*=\left(\mu+\frac{\tau}{2}\right)j. \tag{2.7}$$

In this research, $Q=\left(-\Delta H\right)RA$ represents the heat of chemical reaction which is known as activation enthalpy, where $R_A=K_re^{\frac{E_A}{R_GT}}C^n$ indicates the Arrhenius irreversible reaction (*n*th order), RG indicates the constant of gas (universal), EA represents the energy (activation) and Kr represents the chemical reaction rate. The thermophoresis in Eq. (2.4) can be reported according to Tsai [29] as

$$V_T=-\frac{K^{Th}}{T_{ref}}\cdot\frac{\partial T}{\partial y}, \tag{2.8}$$

where K^{Th} represents the thermophoretic coefficient ranging in values (0.2-1.2) as mentioned by [30].

The binary mixture fluid density and buoyancy term may be introduced as follows:

$$\rho=\rho_\infty\left[1-\beta\left(T-T_\infty\right)\right], \tag{2.9}$$

$$g\left(\rho-\rho_\infty\right)=-g\beta\rho_\infty\left(T-T_\infty\right). \tag{2.10}$$

The pressure term (Buoyancy force) is now expressed as $-\frac{\partial p}{\partial x}=g\rho_\infty\left(T-T_\infty\right)$. In addition, the Boussinesq approximation for combined thermal-mass transfer convection is

$$-\frac{\partial p}{\partial x}=g\beta\rho_\infty\left(T-T_\infty\right)+g\beta\rho_\infty\left(C-C_\infty\right). \tag{2.11}$$

Two cases have been considered in this research $\theta_w=0.1$ and 1.5. The temperature of the mixture $T\left(y,t\right)$ may be represented as $T\left(0,t\right)=T_w$ and $T\left(0,t\right)\to T_\infty$ where dimensionless wall temperature (Pal and Mondal [31]) is assumed. Non-dimensional surface temperature ($\theta_w<1$) usually indicates $T_w<T_\infty$. To find the effect of temperature dependent viscosity; stress should be given on source temperature inside the mixture domain. Consequently, Boussinesq's approximation should be edited for variable viscosity and momentum equation. In the event of mixture's variable viscosity, $\theta_w=0.1$ is just substantial when Eq. (2.11) is edited as

$$-\frac{\partial p}{\partial x} = g\beta\rho_\infty\left(T - T_\infty\right) + g\beta^*\rho_\infty\left(C - C_\infty\right). \tag{2.12}$$

The variable viscosity model introduced by Batchelor [32], accepted by Mukhopadhyay [33] and Animasaun and Oyem [34] can be included as

$$\mu(T) = \mu^*\left[1 + b\left(T_w - T\right)\right],$$

which is only tenable when $T_w > T_\infty$ and is also modified to

$$\mu(T) = \mu^*\left[1 + b\left(T_\infty - T\right)\right], \tag{2.13}$$

and is now tenable when $T_w < T_\infty$.

Applying Eqs. (2.12) and (2.13) in Eq. (2.2), we obtain

$$\frac{\partial u}{\partial t} + v\frac{\partial u}{\partial y} = \frac{1}{\rho}\frac{\partial}{\partial y}\left(\mu\frac{\partial u}{\partial y}\right) + \frac{\tau}{\rho}\frac{\partial^2 u}{\partial y^2} + \frac{\tau}{\rho}\frac{\partial N}{\partial y} + g\beta\left(T_\infty - T\right) + g\beta^*\left(C_\infty - C\right) - \frac{\sigma B_0^2}{\rho}u. \tag{2.14}$$

Eq. (2.3) implies that,

$$\rho C_p\left(\frac{\partial T}{\partial t} + v\frac{\partial T}{\partial y}\right) = \kappa\frac{\partial^2 T}{\partial y^2} + Q - 4\sigma\alpha^2 T^4. \tag{2.15}$$

Using Eq. (2.12), Eq. (2.4) becomes

$$\frac{\partial C}{\partial t} + v\frac{\partial C}{\partial y} + \frac{\partial}{\partial y}\left[V_T\left(C_\infty - C\right)\right] = D_m\frac{\partial^2 C}{\partial y^2} - R_A. \tag{2.16}$$

Using the Eqs. (2.7) and (2.5) becomes

$$\frac{\partial N}{\partial t} + v\frac{\partial N}{\partial y} = \left[\frac{\mu(T)}{\rho} + \frac{\tau}{2}\right]\frac{\partial^2 N}{\partial y^2} - \frac{\tau U_0}{\mu(T)}\left(2N + \frac{\partial u}{\partial y}\right). \tag{2.17}$$

The boundary conditions for Eqs. (2.14)-(2.17) are as:

$$u(y,0) = 0, \quad T(y,0) = T_w, \quad N(y,0) = 0, \quad C(y,0) = C_w, \quad \text{for } t \le 0, \tag{2.18}$$

$$u(0,t) = 0, \quad T(0,t) = T_w, \quad N(0,t) = m_o\frac{\partial u}{\partial t}, \quad C(0,t) = C_w, \quad \text{for } t > 0, \tag{2.19}$$

$$u(\infty,t) \to U_0, \quad T(\infty,t) \to T_\infty, \quad N(\infty,t) \to 0, \quad C(\infty,t) \to C_\infty, \quad \text{for } t > 0, \tag{2.20}$$

the above boundary conditions are valid when $T_w < T_\infty$ and $C_w < C_\infty$.

In Eq. (2.19) when $m_0 = 0$, we have $N(0,t) = 0$. It means microelements in a concentrated substance of the fluid adjacent to the wall as if flows cannot spin.

Upon introducing the following dimensionless variables

$$\eta = \frac{y}{2\sqrt{vt}}, \quad f(\eta) = \frac{u}{u_0}, \quad \varphi = \frac{C}{C_\infty}, \quad N = \frac{U_0}{\sqrt{vt}}h(\eta). \tag{2.21}$$

The mathematical problems defined in Eqs. (2.14)-(2.17) are then transferred into the following set of ordinary differential equations:

$$\left(1 + \xi - \theta\xi + k_1\right)f'' + \xi\theta' f' + 2\left(\eta + c\right)f' + 2k_1 h' + Gr\xi\left(1 - \theta\right) + Gc\xi\left(1 - \varphi\right) - Mf = 0, \tag{2.22}$$

$$\theta'' + 2Pr\left(\eta + c\right)\theta' + Prh_q \times Da \times e^{\omega\left(\frac{\theta-1}{\theta}\right)} \times \phi^n - \Pr Ra\theta^4 = 0, \tag{2.23}$$

$$\varphi'' + 2Sc\left(\eta + c\right)\varphi' + \lambda Sc\left(1 - \varphi\right)\theta'' + \lambda Sc\theta'\varphi' - ScDae^{\omega\left(\frac{\theta-1}{\theta}\right)}\varphi^n = 0, \tag{2.24}$$

$$\left(1 + \xi - \theta\xi + \frac{k_1}{2}\right)h'' + 2\left(\eta + c\right)h' + 2h - \frac{8L_1}{1 + \xi - \theta\xi}h - \frac{2L_1}{1 + \xi - \theta\xi}f' = 0. \tag{2.25}$$

We obtained the dimensionless boundary conditions which are given below:

$$f(\eta)=0,\theta(\eta)=\theta_w(<1),h(\eta)=-\frac{1}{4}f'(0),$$
$$\varphi(\eta)=\varphi_w(<1) \text{ at } \eta=0, \quad (2.26)$$

$$f(\eta)\to 1,\theta(\eta)\to 1,h(\eta)\to 1,\varphi(\eta)\to 1$$
$$\text{as } \eta\to\infty. \quad (2.27)$$

Here η is the similarity variable, $Gr=\frac{4tg\beta}{U_0 b}$ is the modified thermal Grashof number, $\xi=bT_\infty$ is the variable viscosity parameter, $k_1=\frac{\tau}{\mu}$ is the micro-rotation, $Gc=\frac{4tg\beta^*}{U_0 b}$ is the modified solutal Grashof number, $Da=4tK_r e^{-\frac{E_A}{T_\infty R_G}C_\infty^{n-1}}$ is Damköhler number, $h_q=\frac{(-\Delta H)C_\infty}{\rho C_p T_\infty}$ is the heat generation, $Ra=4t\frac{4\sigma\alpha^2T^4}{\rho C_p T_\infty}$ is the radiation, $Pr=\frac{\nu}{\gamma}=\frac{\mu C_p}{\kappa}$ is the Prandtl number, $M=\frac{4\sigma B_0^2 L_1}{\rho k_1 U_0}$ is the magnetic field, $\omega=\frac{E_A}{T_\infty R_G}$ is the activation energy, $L_1=k_1U_0t$ is the time dependent micro-rotation, $\lambda=-\frac{\kappa Th T_\infty}{\nu T_{ref}}$ is the thermophoresis and $Sc=\frac{\nu}{D_m}$ is the Schmidt number, respectively.

3. Numerical Procedure

An investigation for unsteady convective heat and mass transport by micropolar binary mixture passing an upright permeable surface has been carried out to examine the impacts of radiative heat transfer, thermophoresis and chemical reaction with consistent magnetic intensity. For the present analysis, firstly, the nonlinear partial differential Eqs. (2.1)-(2.5) are transformed into second order simultaneous partial differential equations using modified Boussinesq's approximation and then further converted into IVP by using the similarity method. Finally, the obtained IVP involving the set of nonlinear ODEs (2.22)-(2.25) with necessary border situations (2.26)-(2.27) is solved numerically by applying the shooting procedure through "ODE45 MATLAB" software. The range of pertinent parameters in this research is included in the Table 1.

Table 1. Pertinent parameters and their range.

Parameters	Range
Magnetic intensity	0-0.2
Damköhler number	0.05-2
Thermophoresis	0-6
Viscosity	1-4
Radiative heat transfer	0-0.5
Thermal-solutal buoyancy force	-1-2
Prandtl number	0.71-10
Schmidt number	0.22-1

4. Results and Discussion

By using the aforementioned numerical procedure, a parametric study is performed to explore the effects of various non-dimensional parameters/numbers on the non-dimensional velocity, temperature, concentration and micro-rotation characteristics against the dimensionless coordinate η. The results of numerical computation with the variations of these parameters controlling the flow phenomena are presented through graphs 2 to 9. The parameters or numbers involved here are magnetic parameter (M), Damköhler number (Da), thermophoretic parameter (λ), variable viscosity parameter (ξ), thermal radiation parameter (Ra),

modified thermal and solutal Grashof numbers (Gr and Gc), Prandtl number (Pr) and Schmidt number (Sc).

It is mentioned here that, while observing the effect of one parameter or number on the field variables, only the variation of that selected parameters or numbers is made and rest of the parameters or numbers are kept constant values. The constant values of the parameters or numbers are $M = 0.1$, $Da = 0.05$, $Pr = 0.71$, $Sc = 0.22$, $\lambda = 1$, $\xi = 3$, $Ra = 0.2$, $Gr = Gc = 1$. Besides, through the whole numerical calculations the parameters are considered to be fixed. All graphs here are therefore corresponding to these fixed values unless otherwise specified. Also, the boundary conditions at infinity are imposed at a finite point of $\eta = 5$.

4.1 Effect of magnetic field

Fig. 2 depicts the impact of magnetic parameter (M) on the velocity profile. It is observed from the figure that the increasing values of M lead to a decrease in the velocity fields. This is due to the fact that a transversely applied magnetic force produces a Lorentz force which acts like a drag force to slow down the motion of the fluid. Therefore, as the values of M increase, resistive force is also increased resulting in a reduction of the velocity profiles. It is further seen that velocity profiles are found to increase with η and attain to their maximum peak within $1.1 \leq \eta \leq 1.6$ and after that tend to 1 asymptotically as $\eta \to 5$.

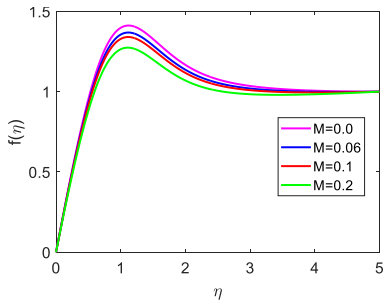

Fig. 2. Velocity profile against magnetic intensity with $Da = 0.05$, $Pr = 0.71$, $Sc = 0.22$, $\lambda = 1$, $\xi = 3$, $Ra = 0.2$, $Gr = Gc = 1$.

4.2 Effect of Damköhler number

The variation of Damköhler number (Da) on the velocity and temperature profiles is drawn in Fig. 3(a-b). A negligible decrease in the velocity close to the wall ($0 \leq \eta \leq 0.95$) is found with the increase of Da but as η increases, velocity enhances significantly with the increasing values of Damköhler number (Da). It is mentioned here that $Da > 0$ represents an increase in the destructive chemical reaction rate.

As is seen in Fig. 3(b), temperature profiles reduce with the decreasing value of Da for the case of destructive chemical reaction (i.e. for $Da > 0$). As Da is the ratio of chemical reaction rate to the heat transfer, a decreasing value of Da indicates the increasing of heat transfer and as a result the temperature profiles decrease. It is natural in process of all exothermic reaction where the heat energy is evolved that enhances the fluid temperature.

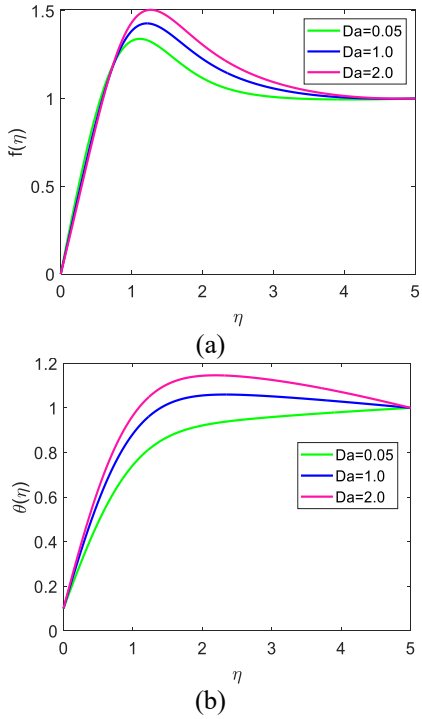

Fig. 3. (a) Velocity, and (b) temperature profiles against Damköhler number with $M = 0.1$, $Pr = 0.71$, $Sc = 0.22$, $\lambda = 1$, $\xi = 3$, $Ra = 0.2$, $Gr = Gc = 1$.

4.3 Effect of thermophoresis

Fig. 4(a-b) illustrates the velocity and concentration distributions within the boundary layer for various values of thermophoretic parameter (λ). It is found that with the increasing value of parameter λ, the momentum boundary layer thickness reduces and hence the velocity reduces.

It is observed from Fig. 4(b) that the species concentration of the fluid increases with the increasing values of λ. A small change in the thermophoresis parameter leads to rapid motion in the fluid particles creating excess heat energy and leading to a massive increase in the concentration distribution. With an increase in the magnitude of thermophoretic parameter, the species concentration through the boundary layer also increased.

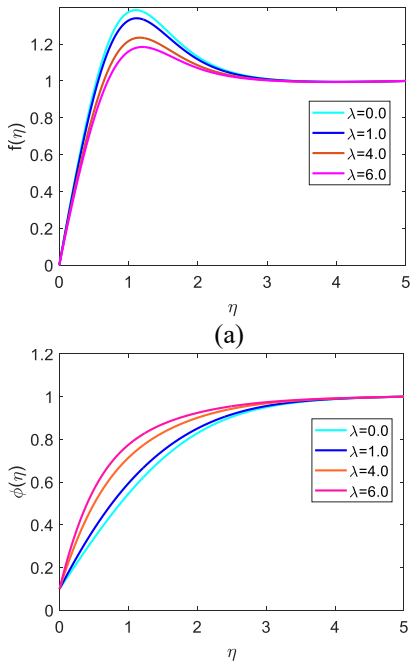

Fig. 4. (a) Velocity, and (b) concentration profiles against thermophoresis with $Da = 0.05$, $Pr = 0.71$, $Sc = 0.22$, $M = 0.1$. $\lambda = 1$, $\xi = 3$, $Ra = 0.2$, $Gr = Gc = 1$.

4.4 Effect of viscosity

Fig. 5(a-b) presents the velocity and micro-rotation profiles for various values of temperature dependent dynamic viscosity ξ. As ξ enhances, the velocity profiles tend to enhance to attain its maximum value closed to the surface $(1 \le \eta \le 2)$ and after that each profile tends to satisfy the far field boundary conditions asymptotically. For constant values of b, the increase of ξ means to increase the amount of input temperature from the free stream into the micropolar fluid domain. When the fluid becomes heated, its intermolecular force is weakened, and the molecules become excited and start moving. The energy of this movement allows the fluid to move faster where the viscosity of the fluid decreases gradually away from the wall and as a result, the velocity enhances from the wall $(\eta = 0)$ to the free stream $(\eta = 3.6)$ with the increasing value of ξ. Thereafter $(3.8 \le \eta \le 5)$ the velocity profiles are not influenced with the increasing value of ξ.

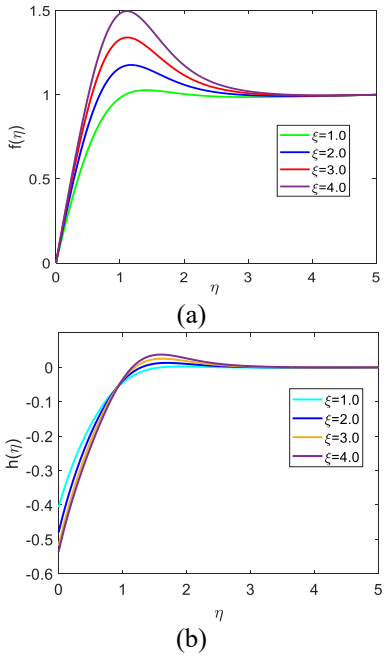

Fig. 5. (a) Velocity, and (b) micro-rotation profiles against variable viscosity with $Da = 0.05$, $Pr = 0.71$, $Sc = 0.22$, $M = 0.1$. $\lambda = 1$, $\xi = 3$, $Ra = 0.2$, $Gr = Gc = 1$.

From Fig. 5(b) the micro-rotation of the particles in the fluid decreases significantly with the increase of ξ, very near to the wall $0 \le \eta \le 1$. But an alternate behavior is observed when $1 \le \eta \le 3.5$ thereafter. Here the micro-rotation profile through the boundary layer increases slightly with the increase of ξ and leads to zero asymptotically as $\eta \to 5$. This is due to the fact that when vortex viscosity depends on temperature only, the micro-rotation of the particles close to the vertical permeable surface will increase. As a result, viscosity of the fluid near the vertical permeable wall will increase. Here the particles within the micropolar fluid region are able to rotate faster. This result is very significant, since the heat energy generated by increasing ξ will affect greatly within a small distance from the wall.

4.5 Effect of thermal radiation

Fig. 6(a-b) shows the impact of thermal radiation parameter (*Ra*) on the velocity and temperature profiles. Since the radiation parameter identifies the relative contribution of conduction heat transfer to thermal radiation transfer, an increase in *Ra* leads to an increase of temperature resulting a decrease of viscosity and increase of velocity of within the boundary layer.

Fig. 6(b) exhibits the temperature profiles for various values of the thermal radiation parameter (*Ra*) which identifies the relative contribution of conduction heat transfer to the transfer of thermal radiation. From the figure, it is noted that when *Ra* increases, the thermal boundary layer thickness of the fluid increases which leads to an increase in the temperature. It is observed that an increase in the radiation parameter increases the temperature within the boundary layer. As the radiation parameter (*Ra*) increases, the temperature also increases which decreases the viscosity within the boundary layer and increases the velocity field.

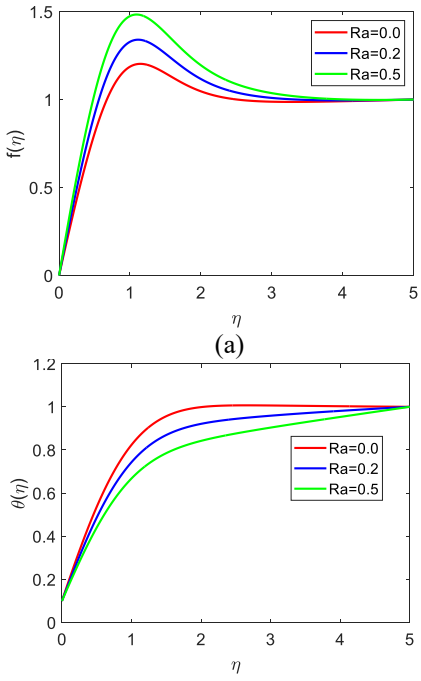

Fig. 6. (a) Velocity, and (b) temperature profiles against radiation with $Da = 0.05$, $Pr = 0.71$, $Sc = 0.22$, $M = 0.1$. $\lambda = 1$, $\xi = 3$, $Gr = Gc = 1$.

4.6 Effect of Grashof number

Fig. 7(a-b) exhibits the impact of local thermal as well as solutal Grashof number (*Gr* and *Gc*) which are termed as the buoyancy parameters on the velocity field. Generally, $Gr < 0$ implies the heating of the surface whereas $Gr > 0$ corresponds to cooling of the surface. In addition, $Gc > 0$ indicates that the surface chemical species concentration is greater than the chemical species concentration in the free stream region whereas $Gc < 0$ concludes that the chemical species concentration at the free stream region is greater than that of the wall. From the figure we observe that when the mode of cooling is increased, the velocity also increases but a converse effect is observed for the case of heating. A similar situation is found for $Gc > 0$ and $Gc < 0$, respectively. It is also well established that the increase of buoyancy parameters enhances the fluid flow.

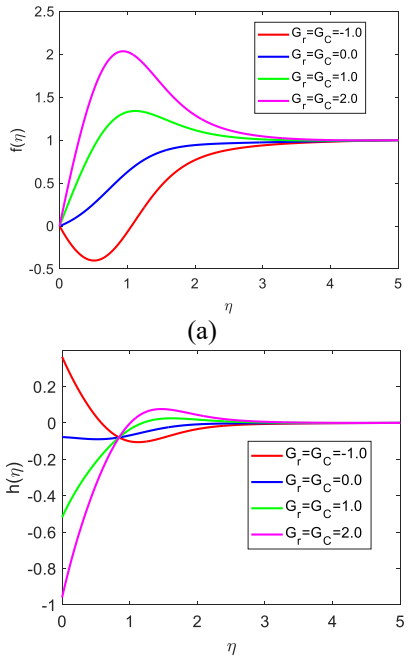

Fig. 7. (a) Velocity, and (b) micro-rotation profiles against thermal and solutal Grashof numbers with $Da = 0.05$, $Pr = 0.71$, $Sc = 0.22$, $M = 0.1$. $\lambda = 1$, $\xi = 3$, $Ra = 0.2$.

The effects of local thermal and solutal Grashof number Gr and Gc on the micro-rotation distributions are found in Fig. 7(b). As they increase from zero to positive values, the micro-rotation of the fluid particles decreases from negative side near the wall in the region $0 \le \eta \le 0.97$. Thereafter a positive trend is observed and asymptotically approaches 1 from the positive side. When Gr and Gc have negative values, a reverse behavior of the above is found. Hence, fluid within the domain highly affects the micro-rotation profiles.

4.7 Effect of Prandtl number

The change of the dimensionless temperature against η for various values of the Prandtl number (P_r) is illustrated in Fig. 8(a-b). From the graph it is noticed that the temperature reduces with the increasing value of Pr for a fixed value of η. Since a higher Prandtl number has comparatively low thermal conductivity, it lessens conduction of heat and therefore, temperature diminishes. Hence, the rate of heat transfer increases due to the increase in magnitude of P_r so that the temperature profiles reduce.

The micro-rotation profile in Fig. 8(b) is found to increase noticeably very adjacent to the surface $0 \le \eta \le 1$ and further than its effect is very tiny even negligible as η increases. Prandtl number has comparatively low thermal conductivity, it lessens conduction of heat and therefore, temperature diminishes. Hence, the rate of heat transfer increases due to the increase in magnitude of Prandtl number so that the temperature profiles reduce. An increase in the radiation parameter leads to an increase in temperature within the boundary layer.

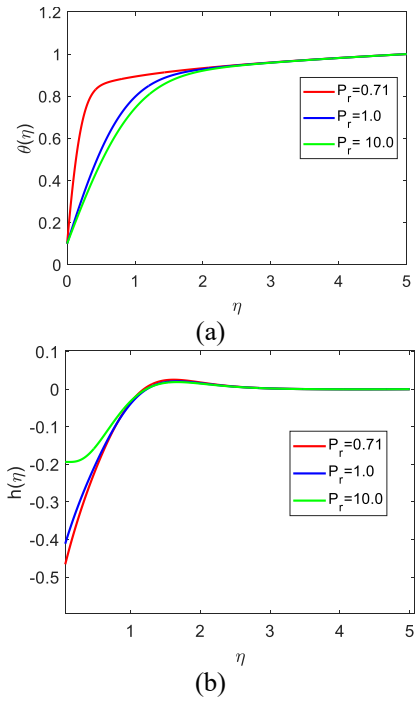

Fig. 8. (a) Temperature, and (b) micro-rotation profiles against Prandtl number with $Da = 0.05$, $Pr = 0.71$, $Sc = 0.22$, $M = 0.1$. $\lambda = 1$, $\xi = 3$, $Ra = 0.2$, $Gr = Gc = 1$.

4.8 Effect of Schmidt number

The impacts of Schmidt number (Sc) on the species concentration and micro-

rotation profiles are observed in Fig. 9(a-b). From this figure it is noticed that an increase of *Sc* leads to a thinning concentration boundary layer and hence the concentration profiles decrease. As the higher values of *Sc* represent heavier species, an increase of *Sc* lowers down the concentration level in the boundary layer. This is due to the fact that as the Schmidt number (*Sc*) increases due to a reduction of the molecular diffusivity of the chemical species, with the increase of kinematic viscosity, the thickness of the concentration boundary layer shrinks.

Fig. 9(b) is sketched to observe the effects of Schmidt number (*Sc*) on the micro-rotation profiles. The higher value of *Sc* corresponds to a small increase of the micro-rotation profiles in a closed proximity to the wall $0 \le \eta \le 1$ and thereafter they change the behavior and decrease somewhat with increasing *Sc* and finally approach zero asymptotically all together.

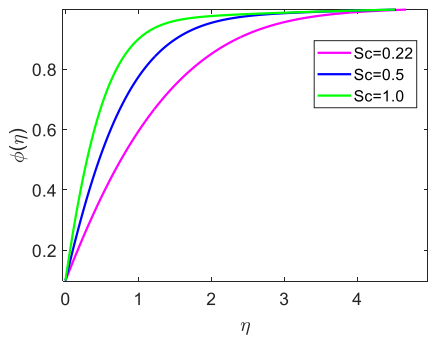

(a)

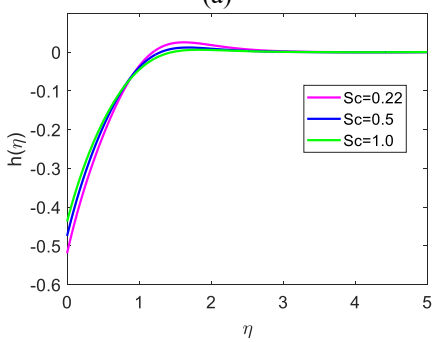

(b)

Fig. 9. (a) Concentration, and (b) micro-rotation profiles against Schmidt number with $Da = 0.05$, $Pr = 0.71$, $M = 0.1$. $\lambda = 1$, $\xi = 3$, $Ra = 0.2$, $Gr = Gc = 1$.

5. Comparison

We compared the numerical results of this study to those of Animasaun [21]. Tables 2 and 3 compare the Nusselt number for the thermal radiation parameter (*Ra*) and the Sherwood number for the Schmidt number (*Sc*) using current numerical results and the published paper. The current numerical results shown in Tables 1 and 2 are discovered to be in good agreement with Animasaun [21].

Table 2. Comparison of local heat transfer rate $-\theta'(0)$ for thermal radiation parameter (*Ra*) applying Classical Runge-Kutta along with shooting technique Animasaun [21] and shooting technique through "ODE45 MATLAB".

Ra	$-\theta'(0)$ [Animasaun [21]]	$-\theta'(0)$ [Present study]	Percentage of error
0.2	-0.9186841	-0.8900077	0.0286765
0.4	-0.8287101	-0.7991377	0.0295725

Table 3. Comparison of local mass transfer rate $-\varphi'(0)$ for Schmidt number (*Sc*) applying Classical Runge-Kutta along with shooting technique Animasaun [21] and shooting technique through "ODE45 MATLAB".

Sc	*c*	$-\varphi'(0)$ [Animasaun [21]]	$-\varphi'(0)$ [Present study]	Percentage of error
0.22	0.0	-0.5827272	-0.5908421	0.0081145
0.42	0.0	-0.8600393	-0.8701159	0.0100765
0.62	0.0	-1.0994216	-1.1097704	0.0103488
0.22	0.5	-0.7980913	-0.7972486	0.0008426
0.42	0.5	-1.2793307	-1.2727648	0.0065659
0.62	0.5	-1.7281449	-1.7142090	0.0139360

6. Conclusions

A numerical investigation of unsteady magneto-convective micropolar binary mixture flow passing an upright permeable

face has been performed under chemical reaction, radiative heat transfer and thermophoresis phenomena. The impacts of different pertinent parameters or numbers on the velocity, temperature, concentration and micro-rotation profiles have been investigated through this research very carefully. The application of findings of this study are significant in the field of heat and mass transfer and thermal science. Important observations regarding the effects of the parameters/numbers on different profiles are as follows:

- The magnetic induction affects the velocity field only in the increase-decrease mode.
- Increases of Damköhler number significantly enhances the velocity fields while interrupt the rate of heat transfer.
- The increasing value of thermophoresis slows down the fluid velocity but improves the concentration distribution massively.
- The temperature dependent dynamic viscosity greatly enhances the velocity of the fluid but reduces the micro-rotation of the particles very near to the wall.
- An increase of thermal radiation enhances both the velocity and temperature within the boundary layer.
- The variation of *Gr* and *Gc* within the region of $0 \le \eta \le 0.95$ highly affects the micro-rotation of the particles.
- The increase of *Pr* lessens conduction of heat while it increases the micro-rotation of the particles noticeably very adjacent to the surface.
- The increase of the value of *Sc* leads to thinning the concentration boundary layer thickness but a small increase of the micro-rotation profiles in close proximity to the wall.

Acknowledgements

This research is carried out in the Department of Mathematics, Khulna University of Engineering and Technology (KUET), Khulna, Bangladesh.

References

[1] Chamkha AJ. Similarity solution for thermal boundary layer on a stretched surface of a non-Newtonian fluid. International communications in heat and mass transfer. 1997 Sep 1;24(5):643-52.

[2] Bird RB. We stewart, and en lightfoot. Transport phenomena. 1960;11:5.

[3] Nasrin R, Alim MA. Combined effects of viscous dissipation and temperature dependent thermal conductivity on MHD free convection flow with conduction and joule heating along a vertical flat plate. Journal of Naval Architecture and Marine Engineering. 2009;6(1):30-40.

[4] Nasrin R, Alim MA. MHD free convection flow along a vertical flat plate with thermal conductivity and viscosity depending on temperature. Journal of Naval Architecture and Marine Engineering. 2009;6(2):72-83.

[5] Sojoudi A, Mazloomi A, Saha SC, Gu Y. Similarity solutions for flow and heat transfer of non- Newtonian fluid over a stretching surface. Journal of Applied Mathematics. 2014 Jan 1;2014.

[6] Ali M, Alim MA, Nasrin R, Alam MS. Study the effect of chemical reaction and variable viscosity on free convection MHD radiating flow over an inclined plate bounded by porous medium. In AIP Conference Proceedings 2016 Jul 12 (Vol. 1754, No. 1, p. 040009). AIP Publishing LLC.

[7] Ali M, Alim MA, Nasrin R, Alam MS. Numerical analysis of heat and mass transfer along a stretching wedge surface. Journal of Naval Architecture and Marine Engineering. 2017 Dec 28;14(2):135-44.

[8] Ali M, Nasrin R, Alim MA. Analysis of boundary layer nanofluid flow over a stretching permeable wedge-shaped surface with magnetic effect. Journal of Naval Architecture and Marine Engineering. 2021 Jun 21;18(1):11-24.

[9] Mohammad Ali, R. Nasrin and M.A. Alim, Axisymmetric boundary layer slip flow with heat transfer over an exponentially stretching bullet-shaped object: A Numerical Assessment, Heliyon, Accepted.

[10] Degan G, Akowanou C, Awanou NC. Transient natural convection of non-Newtonian fluids about a vertical surface embedded in an anisotropic porous medium. International journal of heat and mass transfer. 2007 Nov 1;50(23-24):4629-39.

[11] Kumari M, Jayanthi S. Non-Darcy mixed convection flow of non-Newtonian fluids on a vertical surface in a saturated porous medium. International Journal of Fluid Mechanics Research. 2008;35(5).

[12] Rashad AM, Chamkha AJ, Abdou MM. Mixed convection flow of non-Newtonian fluid from vertical surface saturated in a porous medium filled with a nanofluid. Journal of Applied Fluid Mechanics. 2013; 6(2):301-9.

[13] Lukäszewicz G. Micropolar fluids. Theory and applications, Birkhaüser. Boston, 1999.

[14] Reena R, Rana US. Effect of dust particles on rotating micropolar fluid heated from below saturating a porous medium. Applications and Applied Mathematics: An International Journal (AAM). 2009;4(1):15.

[15] Hinds WC, Zhu Y. Aerosol technology: properties, behavior, and measurement of airborne particles. John Wiley & Sons; 2022 May 24.

[16] Tsai CJ, Lin JS, Aggarwal SG, Chen DR. Thermophoretic deposition of particles in laminar and turbulent tube flows. Aerosol Science and Technology. 2004 Feb 1;38(2):131-39.

[17] Hayat T, Qasim M. Effects of thermal radiation on unsteady magnetohydrodynamic flow of a micropolar fluid with heat and mass transfer. Zeitschrift für Naturforschung A. 2010 Nov 1;65(11):950-60.

[18] Hasanuzzaman M, Sharin S, Hassan T, Kabir MA, Afroj R, Miyara A. Unsteady magneto-convective heat-mass transport passing in a vertical permeable sheet with internal heat generation effect. Transportation Engineering. 2022 Sep 1;9:100126.

[19] Hasanuzzaman M, Azad M, Kalam A, Hossain M. Effects of Dufour and thermal diffusion on unsteady MHD free convection and mass transfer flow through an infinite vertical permeable sheet. SN Applied Sciences. 2021 Dec;3(12):1-1.

[20] Animasaun IL. Effects of thermophoresis, variable viscosity and thermal conductivity on free convective heat and mass transfer of non-darcian MHD dissipative Casson fluid flow with suction and nth order of chemical reaction. Journal of the Nigerian Mathematical Society. 2015 Apr 1;34(1):11-31.

[21] Animasaun IL. Double diffusive unsteady convective micropolar flow past a vertical porous plate moving through binary mixture using modified Boussinesq approximation. Ain Shams Engineering Journal. 2016 Jun 1;7(2):755-65.

[22] Ali M, Alim MA, Nasrin R, Alam MS, Chowdhury MZ. Magnetohydrodynamic boundary layer nanofluid flow and heat transfer over a stretching surface. In AIP Conference Proceedings 2017 Jun 19 (Vol. 1851, No. 1, p. 020022). AIP Publishing LLC.

[23] Ali M, Alim MA, Nasrin R, Alam MS, Munshi MH. Similarity solution of unsteady MHD boundary layer flow and heat transfer past a moving wedge in a nanofluid using the Buongiorno model. Procedia engineering. 2017 Jan 1;194:407-13.

[24] Hossain MM, Nasrin R, Hasanuzzaman M. Radiative effect on unsteady magneto-

convective heat- mass transport by micropolar binary mixture passing a continuous permeable surface. Advances in Mathematical Physics, Accepted.

[25] Cheng P. Two- dimensional radiating gas flow by a moment method. American Institute of Aeronautics and Astronautics Journal. 1964 Sep;2(9):1662-64.

[26] Makinde OD. Free convection flow with thermal radiation and mass transfer past a moving vertical porous plate. International Communications in Heat and Mass Transfer. 2005 Nov 1;32(10):1411-9.

[27] Rahman GM. Effects of magnetohydrodynamic on thin films of unsteady micropolar fluid through a porous medium, 2011. J. Mod. Phys.;2(11):1290-304.

[28] Qasim M, Khan I, Shafie S. Heat transfer in a micropolar fluid over a stretching sheet with Newtonian heating. Plos One. 2013 Apr 2;8(4):e59393.

[29] Tsai R, Chang YP, Lin TY. Combined effects of thermophoresis and electrophoresis on particle deposition onto a wafer. Journal of Aerosol Science. 1998 Aug 1;29(7):811-25.

[30] Batchelor GK, Shen C. Thermophoretic deposition of particles in gas flowing over cold surfaces. Journal of Colloid and Interface Science. 1985 Sep 1;107(1):21-37.

[31] Pal D, Mondal H. MHD non- Darcian mixed convection heat and mass transfer over a non- linear stretching sheet with Soret– Dufour effects and chemical reaction. International communications in heat and mass transfer. 2011 Apr 1;38(4):463-7.

[32] Batchelor GK. An introduction to fluid dynamics. Cambridge university press; 2000 Feb 28.

[33] Mukhopadhyay S. Effects of radiation and variable fluid viscosity on flow and heat transfer along a symmetric wedge. Journal of Applied Fluid Mechanics. 2012 Jan 1;2(2):29-34.

[34] Animasaun IL, Oyem AO. Effect of variable viscosity, Dufour, Soret and thermal conductivity on free convective heat and mass transfer of non- Darcian flow past porous flat surface. American Journal of Computational Mathematics. 2014 Aug 29;4(04):357.

Nomenclature

B_0	magnetic field intensity, Am^{-1}
c	suction parameter
C	particle concentration, kgm^{-3}
C_p	specific heat at constant pressure, kJ $kg^{-1} K^{-1}$
C_w	surface concentration, kgm^{-3}
C_∞	free stream concentration
Da	Damköhler number
D_m	coefficient of mass diffusivity
E_A	activation energy
$f(\eta)$	dimensionless velocity function
g	acceleration due to gravity, ms^{-2}
Gc	modified solutal Grashof number
Gr	modified thermal Grashof number
h_q	heat generation parameter
$h(\eta)$	dimensionless micro-rotation function
K_1	micro-rotation parameter
M	magnetic parameter
MHD	magnetohydrodynamic
N	angular momentum
Pr	Prandtl number
Q	activation enthalpy
q_r	radiative heat flux
Ra	radiation parameter
Re	Reynolds number
R_G	universal gas constant
Sc	Schmidt number
T_w	surface temperature, K
T_∞	free stream temperature
u	velocity component along x axis, ms^{-1}
U_0	uniform velocity at free stream

V_T	thermophoretic velocity
η	similarity variable
$\theta(\eta)$	dimensionless temperature function
κ	thermal conductivity
λ	thermophoretic parameter
μ	dynamic viscosity
ν	kinematic viscosity, m^2s^{-1}
ξ	variable viscosity parameter
ρ	density of base fluid, kg m^{-3}
τ	vortex viscosity
$\varphi(\eta)$	dimensionless concentration function
ω	activation energy parameter